STAR Note # SN260
12 September 1996

Small Prototype of the ENDCAP EMC for STAR. Test Results [1]

Gavrichtchouk O., Eremeev R., Kutuev R., Kouzmine N., Savin I., Zulkarneev R.
Joint Institute for Nuclear Research

Kholodenko A.
Institute for High Energy Physics, Protvino, Russia

[1]Partially supported by the Contract N776734 between BNL and JINR.

Introduction

The Electromagnetic Calorimeter (EMC) [1] is proposed for the Solenoidal Tracker at RHIC (STAR) [2] to increase physics capabilities of the detector both in studying relativistic heavy ion collisions and polarized proton–proton collisions. The Endcap part of the EMC (EEMC) plays a very important role in the pp–collisions enlarging the detector acceptance for processes relevant to the proton spin studies. It is also very useful to the quark–gluon plasma searches.

The EEMC is a proposed contribution from JINR to STAR. Before finalizing its design and starting a construction it is necessary to study the main components. The small prototype (SP) of the EEMC is constructed (section 2) and tested in the beam at Serpukhov (section 3) for these purposes.

The programme of testing included the energy calibration of the modules of the SP in the beam of muons ($E = 1\ GeV$) and electrons ($E = 26.6\ GeV$) as well as using a photo diode technique. This test and additional measurements allowed one to estimate experimentally such important features of the device as:

1. Energy resolution of the modules while registering electrons with the energy of 26.6 GeV;
2. The light output of the scintillators in combination with different types of the WLS–fibers;
3. Influence of the edge effects in the modules on the signal amplitude and energy resolution of the calorimeter.

The work has been partially supported by the Contract N 776734 between BNL and JINR.

1 Small Prototype Construction

1.1 Design

The small prototype of the EEMC is composed of 4 towers, sampling structure of which is similar to that of the full scale prototype of the EEMC being designed at Dubna [4]. The scheme of the SP is given in Fig.1. It consists of 25 layers of the scintillator, with the sizes of $142 \times 146 mm^2$, and absorber made of lead, 5 mm thick. The total thickness of the absorber is approximately 25 $rad.$ long. There is a space in the SP specially reserved to mount SMD, the Shower Max Detector. That is why it is necessary to include into the structure of the small prototype some additional elements destroying its homogeneous sampling:

1. The absorber in the region of SMD made of aluminum, 8 mm thick, and steel 7 mm thick;
2. To increase the rigidity of the construction, the $15th$ layer of the absorber is made of steel, 7 mm thick;
3. The entrance window of the calorimeter made of aluminum, 20 mm thick to imitate the presence of the supporting walls of TPC in front of the end cap.

1.2 Position of the Towers in the Beam

Fig.1 shows the position of the towers (modules: M1, M2, M3, M4) in the beam and gaps between them: – 6.0 mm between M2 and M4; –1.2 mm between M1 and M3; – 0.05 mm between M1 and M4, as well as between M2 and M3.

1.3 Scintillator

The scintillator tiles are manufactured from granulated polystyrene PSM–115 using the method of molding by pressure. Scintillating components:

1. p–terphenile (1.5%) – the primary component with radiation spectrum at the wave length of about 320 mm;
2. POPOP (0.03%) – the secondary component with radiation spectrum at the wave length of 420 nm.

Sizes of the scintillation plates – 142×146 mm^2, 5 mm thick. The plates are wrapped with Tyvek paper, 40 μ thick (only on large sides), and aluminized mylar, 20 μ thick (Fig.2).

Fig.3 shows the results of scanning the scintillator plate with the source of Beta–particles (diameter – 2 mm, energy – 2 MeV) using two fibers for light collection as shown in Fig.2.

1.4 Absorber

The absorber consists of 300×300 mm^2 lead plates, 5 mm thick. The absorber covers 4 modules without gaps between them. The absorber plates were separated from the scintillators through $G10$–material of 2 mm thick to make a free space for the fibers from the neighbouring modules.

1.5 Wavelength Shifting Fibers (WLS)

Three types of WLS fibers, 1.0 mm in diameter, were used in SP. All the fibers have the radiation spectrum at the wave length approximately equal to 520 nm. A certain type of the fibers has been used in each module:

M1 – Y–11 (m.c.) – length 210 cm;
M2 – BCF–91A (s.c.) – length from 120 cm up to 180 cm;
M3 – BCF–91A (m.c.) – length 210 cm;
M4 – BCF–91A (s.c.) – length 180 cm

where m.c. is a multi layer covering, s.c. is a single layer covering.

The fiber was stacked in the form of a loop along two narrow sides of the scintillator (without a groove on the edge). The extra part of the loop was placed on the surface of the neighbouring scintillator shifted by 1.0 mm. The dependence of the signal amplitude on the length of the fibers of different type is shown in Fig.4.

1.6 Photomultiplier (PM)

Russian PM's PHEU–84 having a multi alkaline photo cathode, and the $12th$ cascade dinode system, was used.

The photomultipliers were selected requiring the quantum sensitivity at the wave length of 520 nm to be $(17-18)$ %. The PM quantum sensitivity dependence on the wave length is given in Fig.5. From the distribution of the values of the quantum sensitivity (Fig.6) for 200 pieces of the PHEU–84A, it is seen that the average value is equal to 14.5% with a half width of 4 %.

The selected PM's have been checked for the amplitude stability to the frequency loading in the range up to 2 MHz (at the yield of the order of 1000 photo electrons). The instability was less than 4 %.

The voltage divider was resistive (non–uniform with voltage increasing on the last dinodes). The current through the divider was in average 0.25 mA. The last 4 dinodes were fed from the current autonomous sources.

2 Scheme of Measurements

2.1 The Beam

The measurements of the calorimeter characteristics were carried out in the channel N 2 of U–70 (Protvino) at the energy of the electron beam equal to 26.6 ± 1.1 GeV. The intensity of the electron beam was 10^4 per accelerator cycle. The hadron–muon contamination of the beam is at the level of ~ 0.5 %.

2.2 The layout

The layout of SP and other detectors in the beam is shown in Fig.7. Scintillation counters were used to define the charged particles (Table 1) . The trigger to start the registering electronics was developed by coincidence of the scintillation counters S_1, S_2, S_3, S_5. Counter S_4 was included into the anticoincidence to suppress the halo around the beam. Counter S_μ was used to form the muon label.

The signals from the calorimeter modules were registered by ADC LRS–2249. The trigger gate was equal to 110 ns, its size was determined by the duration of the LED pulse from PM. The duration of the beam particle pulses from PM did not exceed 40 ns.

2.3 Beam Hodoscope

The coordinate of the incoming beam particles was determined at the entrance of the calorimeter with the help of the scintillation hodoscope. It is a 36–channel detector with space resolution of 3.2 mm. The hodoscope consisted of scintillation strips: 3.0 mm wide, 4.0 mm thick and 100 mm long. The light from them was collected on 12 PHEU–85 using the WLS fibers. The working aperture of the hodoscope was equal to $115 \times 100\ mm^2$.

The hodoscope pattern was build using a special coding of discrete elements. All 36 strips were divided into 6 groups, each of 6 strips. The first strips of each group were joint onto one PM, the second–onto another PM and etc. So, the 12 PHEU–85 registered the signals from the 36 discrete elements. The signals from PM were recorded by ADC and further processed off–line.

2.4 Test of the SP with Muons

For these tests the beam line was closed with a shield. The μ–mesons passing through the calorimeter absorber (22 *rad. length*), were selected by the amplitude of the signals from the counter S_μ (Fig.8,a).

The amplitude distribution of the signals from the counter S_5 is shown in Fig.8,b. The separated muons have the energy of about 1 GeV and irradiated the central part of each of the EMC modules. The corresponding amplitude distributions are shown in Fig.9.

The LED calibration spectra are given in Fig.10. They have been used to estimate the number of the photo electrons N_{pe} by the formula:

$$N_{pe} \sim (< A > / \sigma)^2,$$

where $< A >$ is the average amplitude of the spectrum and σ is a mean–square–root deviation.

Value N_{pe} actually is only proportional to the number of the photo electrons but its fluctuation exactly reflects the contribution of the photo statistics into the amplitude (energy) resolution of the detector.

The results of the photo electron number estimations for muons are given in Table 2.

3 Test of the SP with Electrons

For these tests the beam of the particles was directed into the center of each SP module. The amplitude distribution of the pulses from counter S_μ (see Fig.11,a) identified the presence of the shower leakage from the calorimeter. The amplitude distribution of the pulses from counter S_5 was used to identify the multitrack events in the trigger. The second and third peaks in the amplitude distribution of counter S_5 (Fig.11,b) proved the presence of several charged particles passing through the scintillator. Only those events which corresponded to the dashed area in counter S_5 were used for the further analysis.

3.1 Energy Resolution of the Modules

Fig.12 shows the amplitude distribution of the pulse from the calorimeter corresponding to the beam position in the centre of the modules. The multitrack events and γ–background from the beam particles are the reason of appearance of the pulses to the left from the electron peak. Spreading the left side of the peaks in these spectra is evidently caused by an admixture of hadrons in the beam. The side and longitudinal leakages in the calorimeter result in pulse spectrum spreading.

Table 3 gives energy resolution of the calorimeter obtained while irradiating its separate modules. The energy resolution of the present SP at the energy of electrons equal to 26.6 GeV, has a value of 5 $\% \pm 0.3$ % in average for all modules. To estimate the sampling resolution of the SP, the above value should be corrected taking into account the energy spread of the electron beam, equal to 4 %. Inserting this correction gives the value for the sampling resolution 20.4 $\%/\sqrt{(E(GeV))}$.

The abnormally large values $\sigma_E/E = 9.2 \pm 1.2$ for module 2 are explained by nonregularity in the light collection due to different length of the fibers connecting PM's with the scintillators (see Sect. 1.5). It is well known from [3], that this effect gives a linear but not a quadratic contribution into the energy resolution of the calorimeter. In our case the value of this nonregularity is equal to ~ 8 % which fully explains the energy resolution observed in module 2.

3.2 Photo Statistics

The calibration of the PM's was performed with light diodes. The values $N_{pe} \sim (< A > /\sigma)^2$ were measured in the range of the amplitude spectra corresponding to electrons with the energy from 10 to 20 GeV. Fig.13 gives the N_{pe} as a function of energy for each of the SP modules. The linear approximation of N_{pe} vs. energy has given the number of photo electrons per 1 GeV (see Table 3).

The average value of the photo–electrons for all modules is equal to (197 ± 5) $per/$ 1 GeV. The contribution of the photostatistics into the energy resolution of the calorimeter at 26 GeV is 1.4 %.

4 Study of the Calorimeters Edge Effects

4.1 Selection of Events

For these tests the beam hodoscope H was installed at the center of the SP. It provided an opportunity to select the amplitude distribution of the pulses distorted by the "dead" areas:

–at the border of modules 1 and 3 (1.2 mm);

–at the border of modules 2 and 4 (6.0 mm).

While scanning the border lines of the modules – $M1 + M3$ or $M2 + M4$, only those events were selected for the analysis which corresponded to passing the particles through these pairs of the modules.

The edge effects were studied with incoming muons and electrons. The selection of the events was carried out on track multiplicity using the hodoscope. Fig.14 shows the signal spectra from scintillation counters S_μ (a) and S_5 (b) with selection on the track multiplicity. The shadowed and light parts of the spectra obtained with the track multiplicity equal to 1 and 4, correspondingly. The requirement on multiplicity 4 suppresses the background by factor 2.

4.2 Energy Response of the SP at the Modules Border

For electron scanning the trigger scintillation counter S_5 has had sizes $30 \times 50\ mm^2$ permitting the exposition on the module pairs $M1+M3$ or $M2+M4$.

In the muon beam the trigger counter S_5 has had sizes $100 \times 100\ mm^2$ permitting to expose 4 modules simultaneously. The amplitude distributions of the signal sums $M1 + M3$ or $M2 + M4$ for muons and electrons are shown in Fig.15 and 16, respectively.

Table 4 gives deviations of amplitudes from the average one for the signals in the region of the dead areas. For the electron case these deviations do not exceed 12 % even for a large gap of 6 mm.

5 The Calorimeter Response to Hadrons

The amplitude spectrum of one of the modules was also measured in the pions beam with the energy of 40 GeV (see Fig.17). This spectrum had a usual shape.

6 Conclusions

1. The number of photo electrons produced in one scintillation tile of the calorimeter by the minimum ionizing particles was estimated to be

$$N_{pe} = 2,5 \pm 0,4\ .$$

2. It was shown experimentally that the light output of the scintillator, light collection and sensitivity of the PM PHEU–84 used in the model under consideration are high enough to obtain the sampling resolution of the EEMC $\sim 20\ \%/\sqrt{(E)}$.

3. The energy response of the calorimeter was measured in the region close to the border of the two neighbouring towers with the distance of 1.2 and 6.0 mm between them. No significant fall of the response was found in this region for electrons. The deviations from the average amplitude of signals in the dead areas were equal to:

e-beam	mu-beam	Gap, mm
12%±3%	56±13%	6.0
3%±3%	22±5%	1.2

4. The WLS–fibers of the types Y11 or BCF91A (m.c. or s.c.) up to about 200 cm long can be used for the EEMC construction.

Acknowledgements

The authors express their gratitude to the Directorate of the IHEP (Protvino) for the opportunity to work at U–70, to Dr. D.Underwood (ANL, Argonne) for the WLS fibers, the LPP Serpukhov Department group for the participation in the construction of the model and A.P.Meschanin (IHEP, Protvino) for his helpful work.

References

[1] The Electromagnetic calorimeter for the Solenoidal Tracker at RHIC, PUB–5380, (1993).

[2] Conceptual Design Report for Solenoidal Tracker at RHIC(STAR), PUB–5347, (1992).

[3] Energy Resolution of the Lead Scintillating Fiber Electromagnetic Calorimeter. NIM 343A (1994), p.476.

[4] The Endcap Electromagnetic Calorimeter for STAR. Technical design report in preparation.

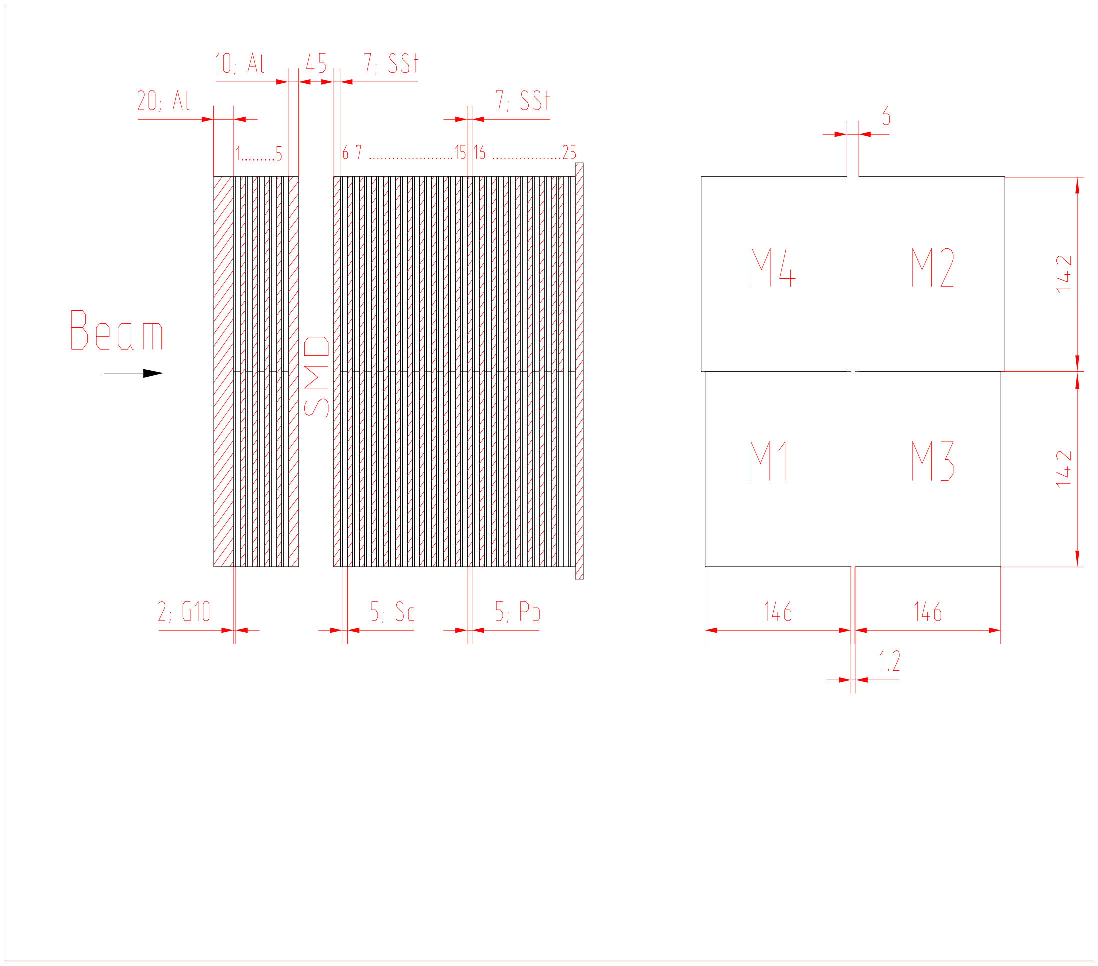

Fig.1. The structure of the SP and an arrangement of modules.

Sc – Plastic scintillator;

Pb – Absorber plate;

Al – Aluminum;

St – Steel;

G10 – Fiberglass;

SMD – The volume for Shower max. detector.

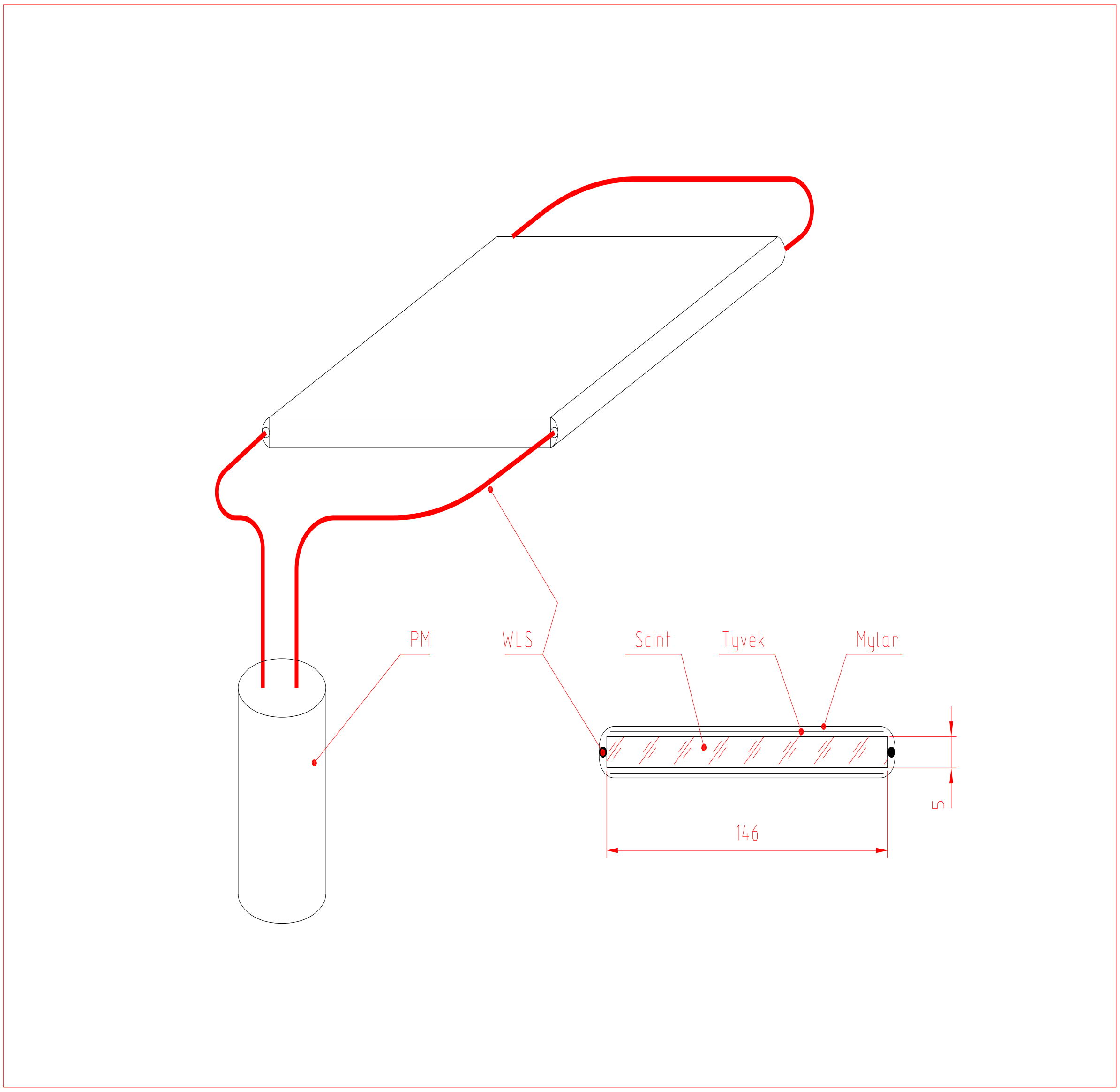

Fig.2. The Scintillator tiles wrapping and WLS fibers;

WLS – a wavelength shifting fibers, 1.0 mm diameter;

Sc – Scintillator tiles;

PM – Photomultiplier;

Tyvek – White paper, thickness 40 microns;

Mylar – Aluminized mylar, thickness 20 microns.

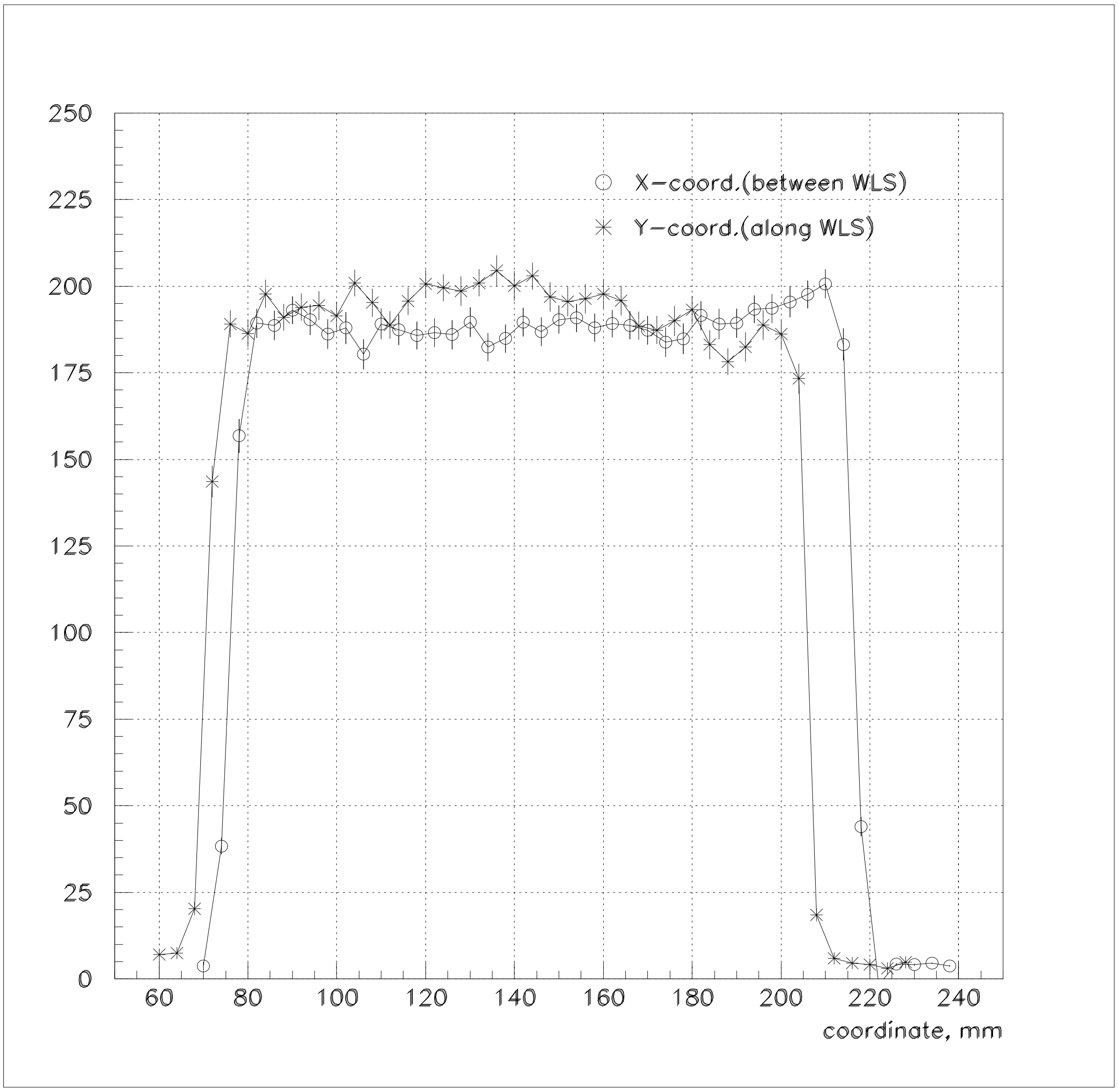

Fig.3. A typical response map of scintillator tiles.

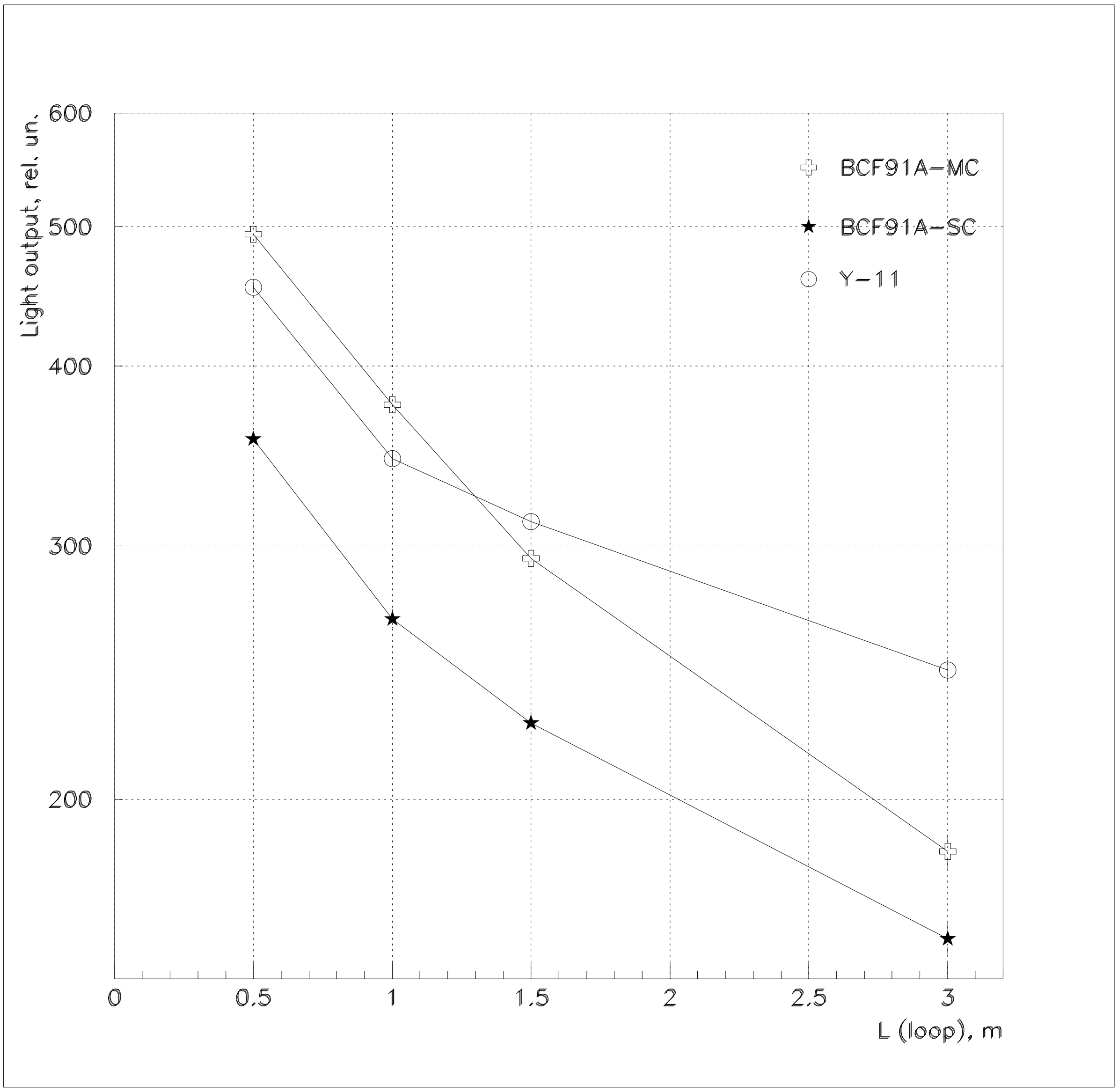

Fig.4. Attenuation length of the WLS fibers.

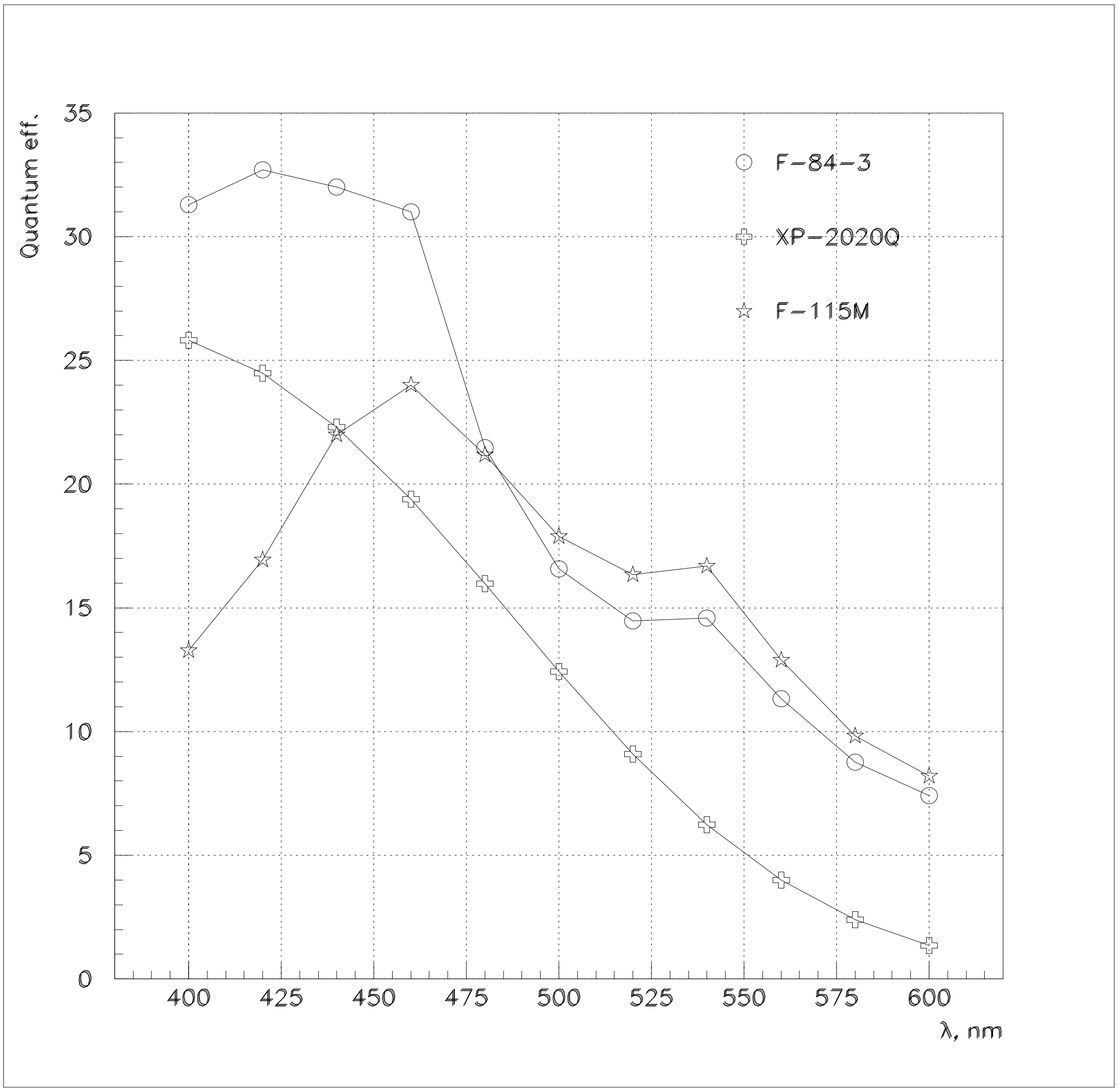

Fig.5. Quantum sensitivity of the PM's.

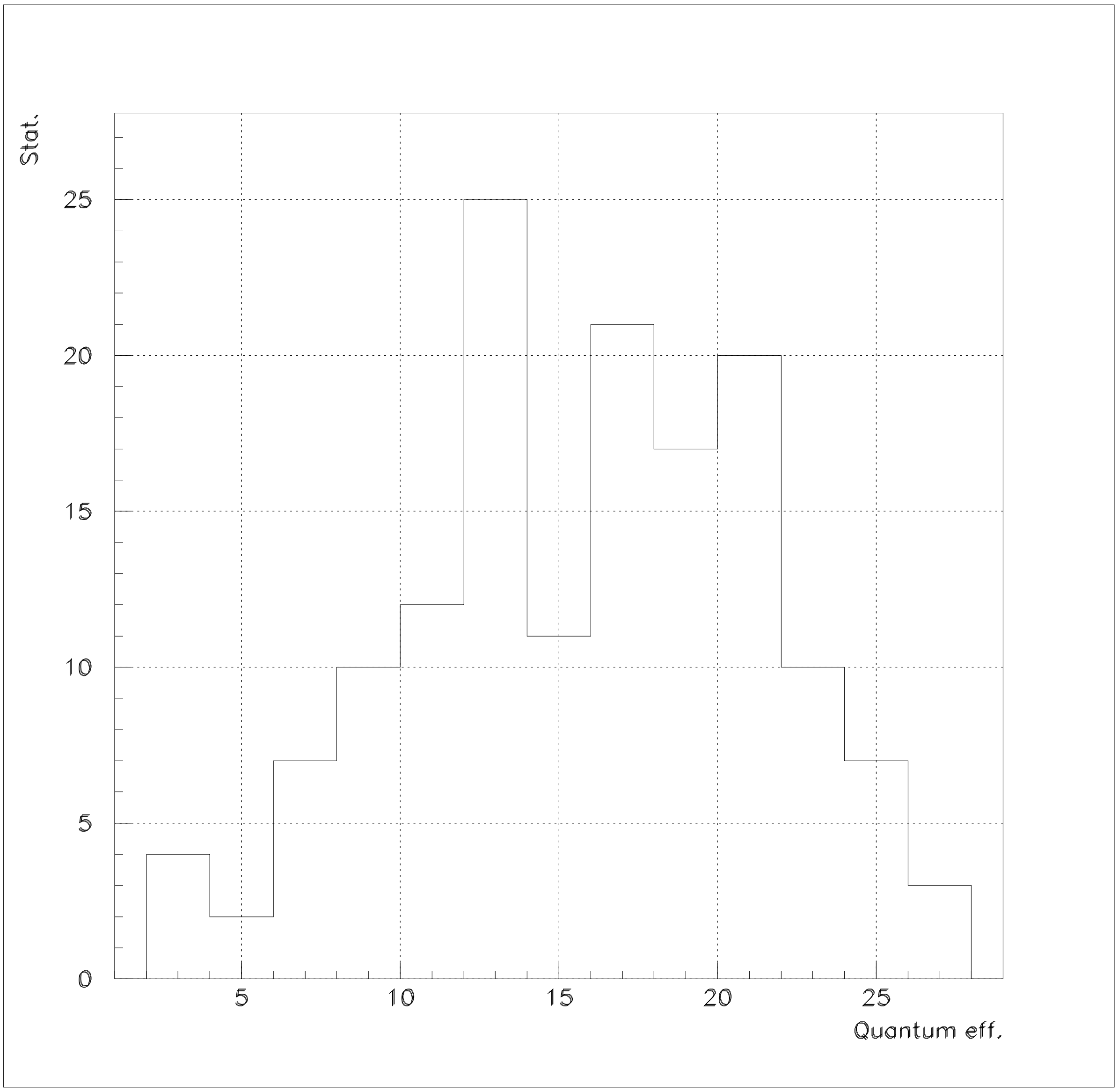

Fig.6. Quantum sensitivity distribution of the PHEU–84.

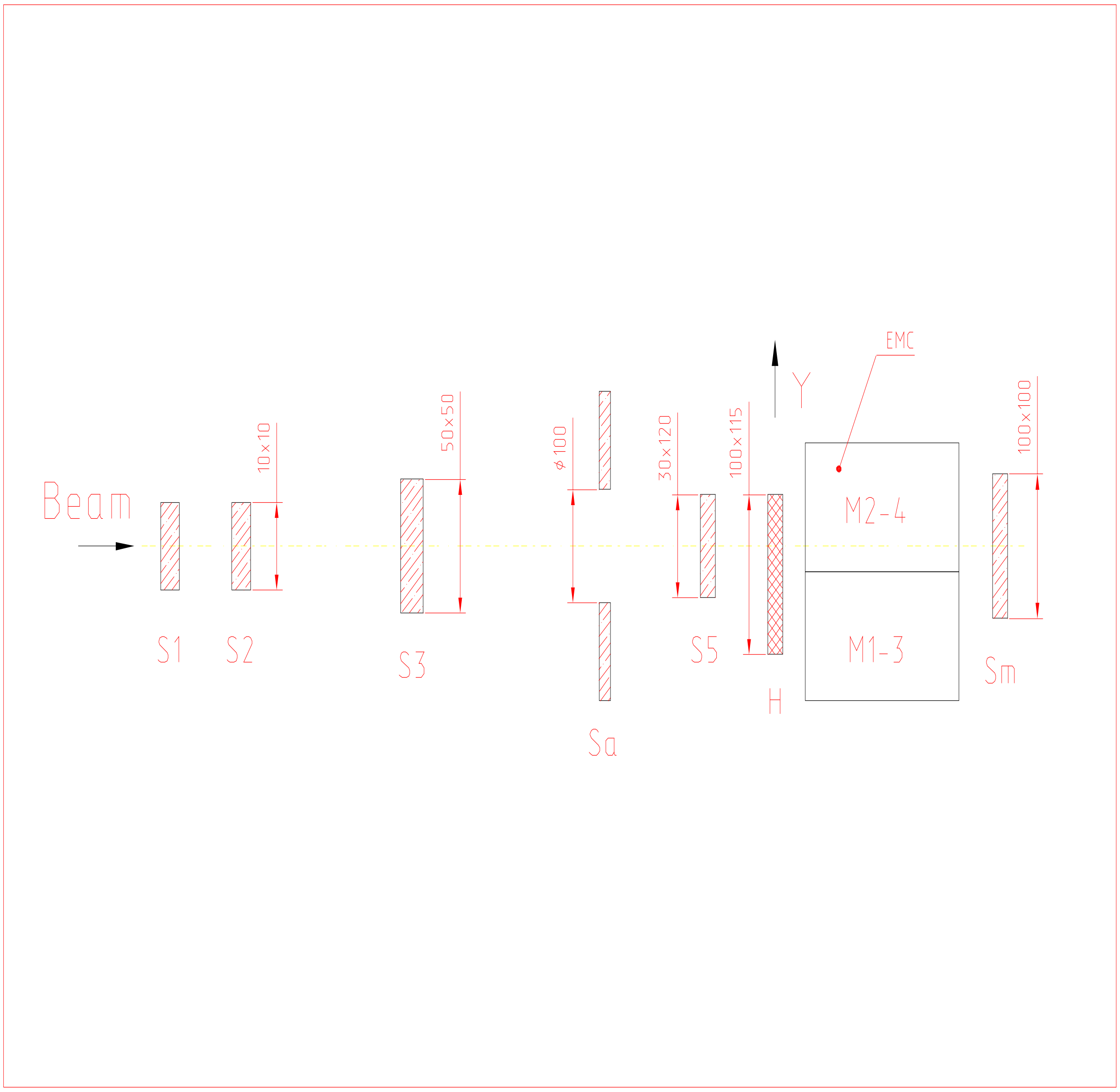

Fig.7. The layout of the detectors in the beam.

S_1, S_2, S_3, S_5, S_A, S_μ – scintillation counters;

H – Scintillation hodoscope;

EMC – The small prototype SP of EMC;

M2–M4, M1–M3 – The modules of SP;

Y – Direction of a vertical axis.

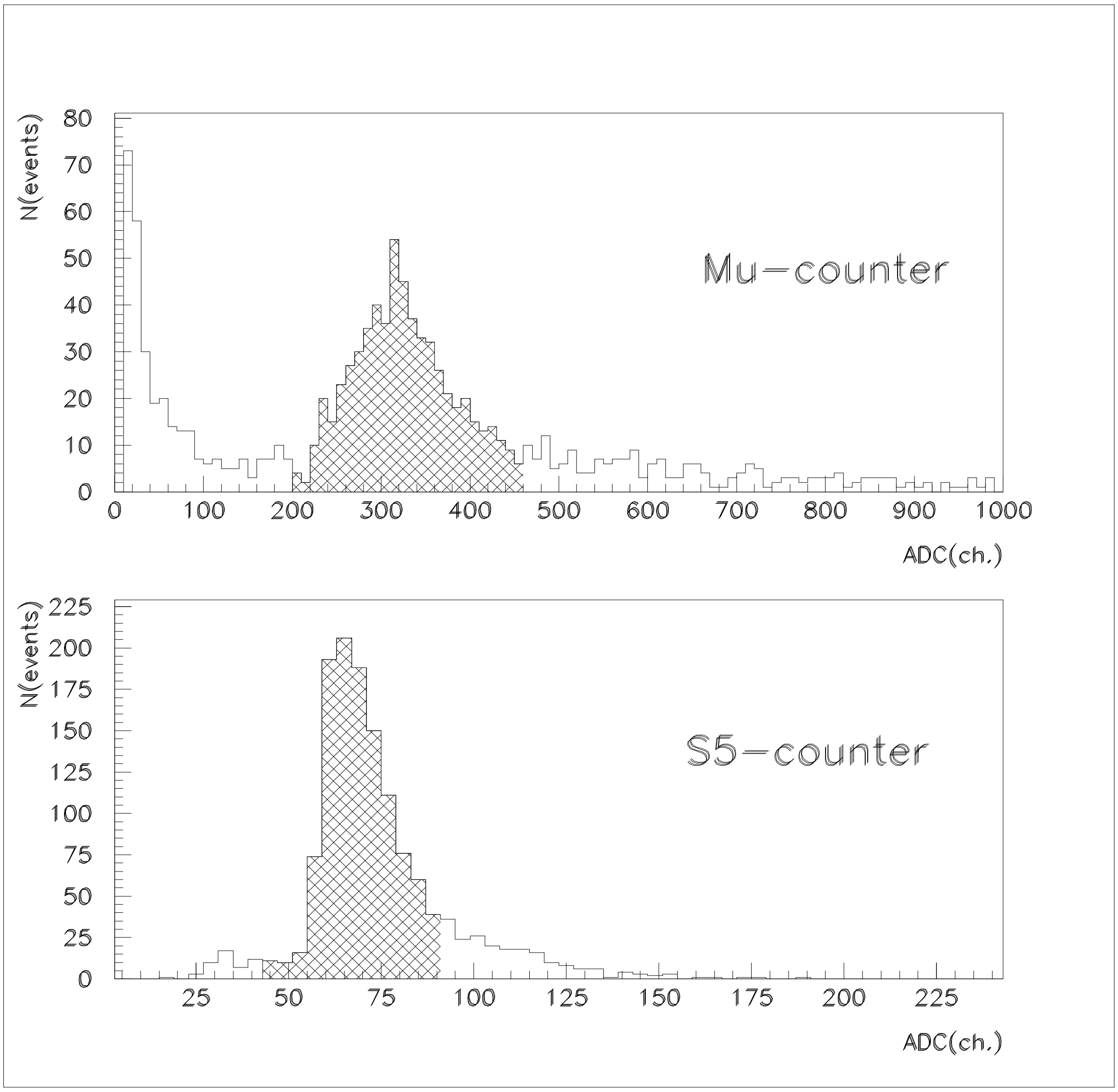

Fig.8. Pulse height distributions for muons and hadrons from $S_\mu(a)$ and $S_5(b)$ counters. Dashed area shows the pulse region for minimum ionization particles.

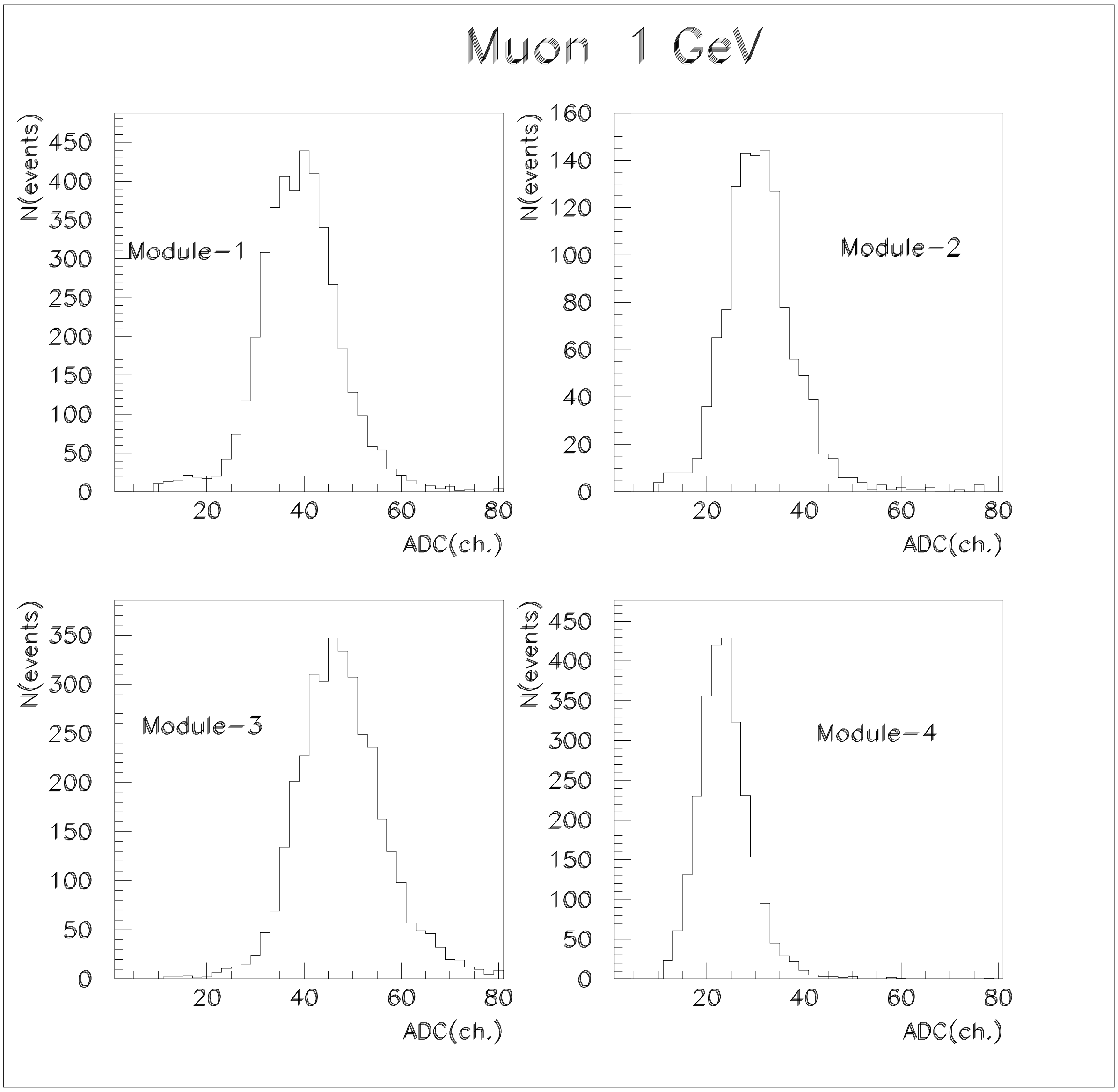

Fig.9. Pulse height distributions for muons in SP modules.

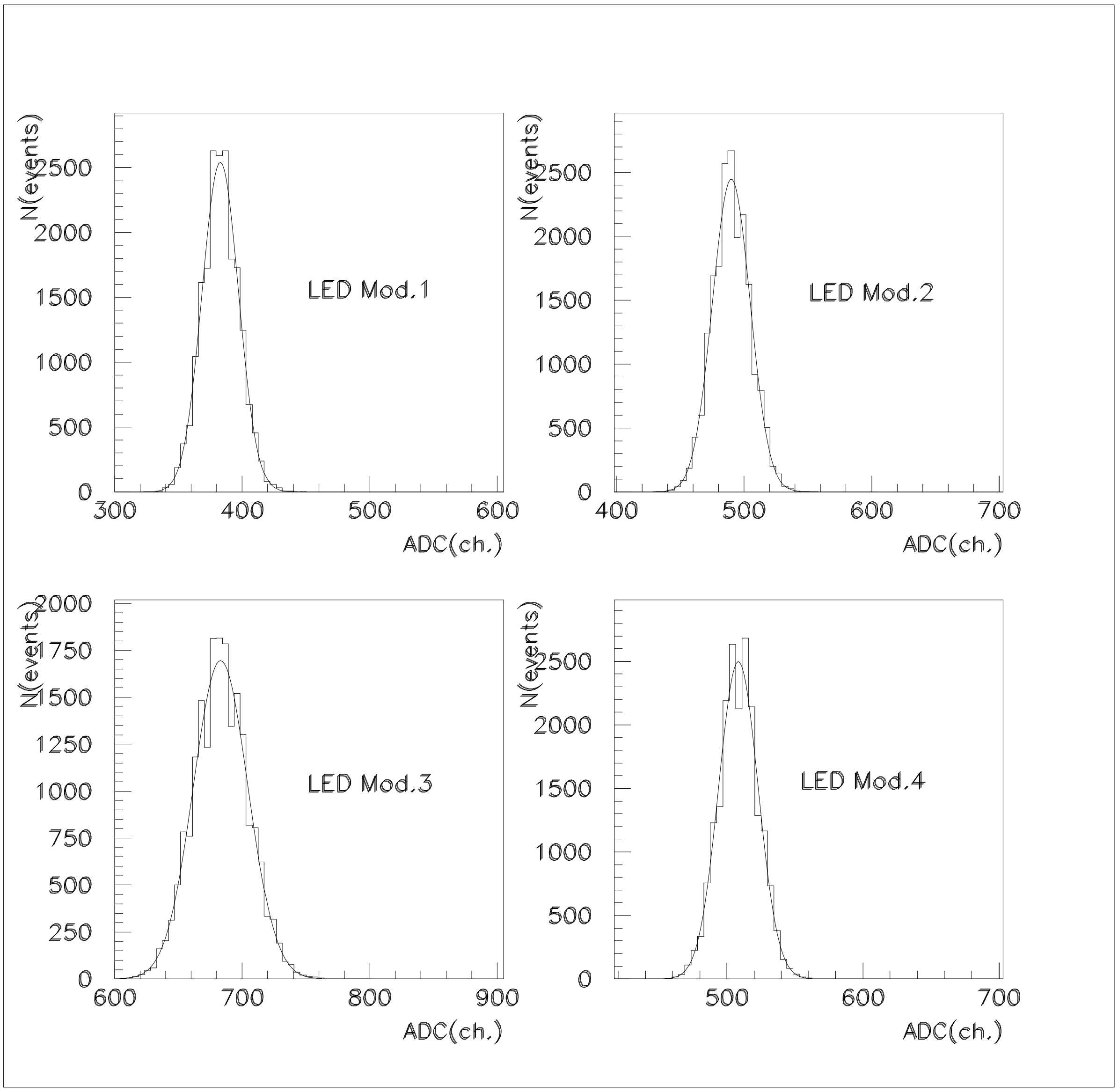

Fig.10. Pulse height distributions from LED in the SP modules.

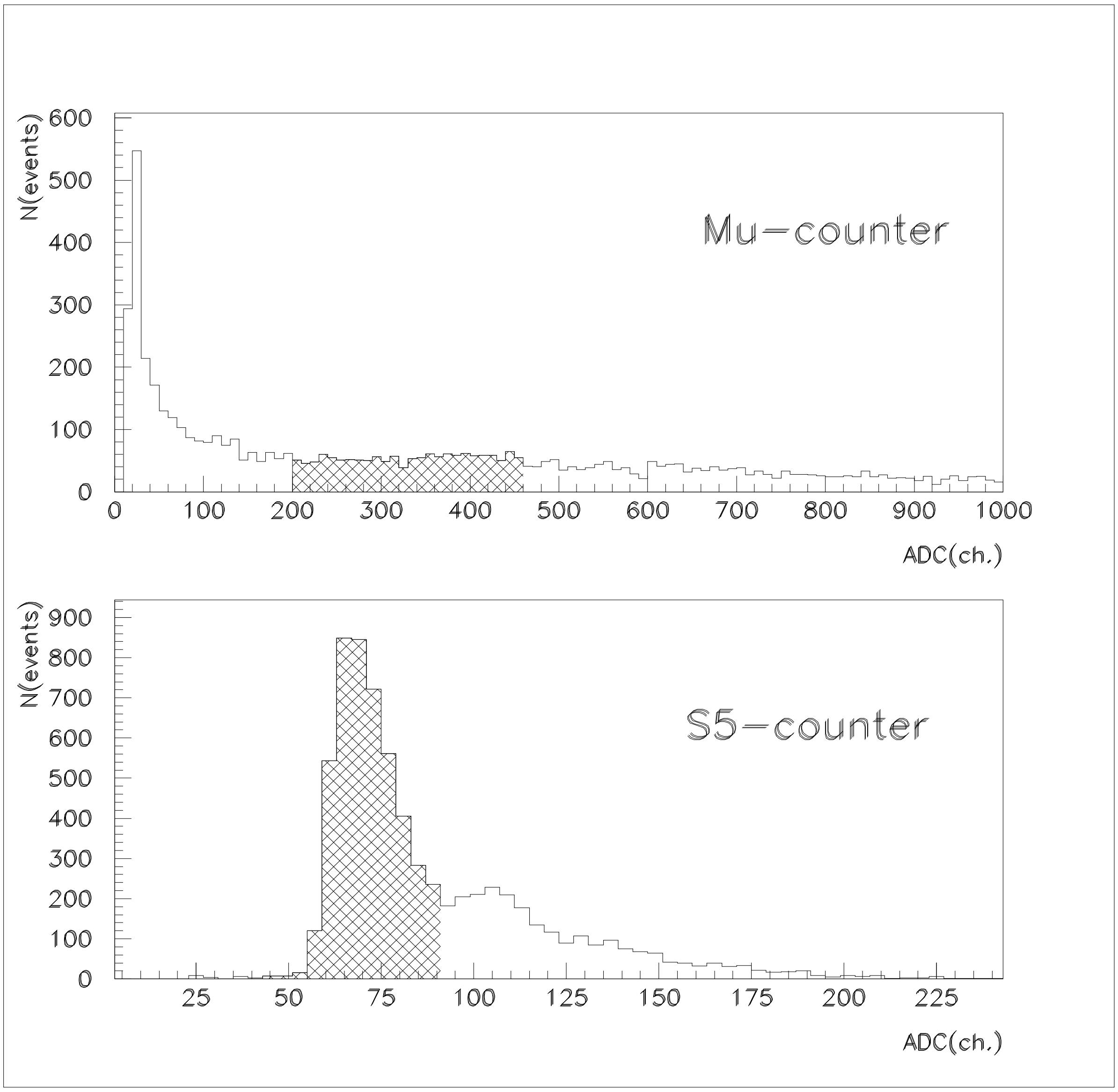

Fig.11. Pulse height distribution for electrons from $S_{\mu}(a)$ and $S_5(b)$ counters. Hatched areas correspond to single minimum ionization particles.

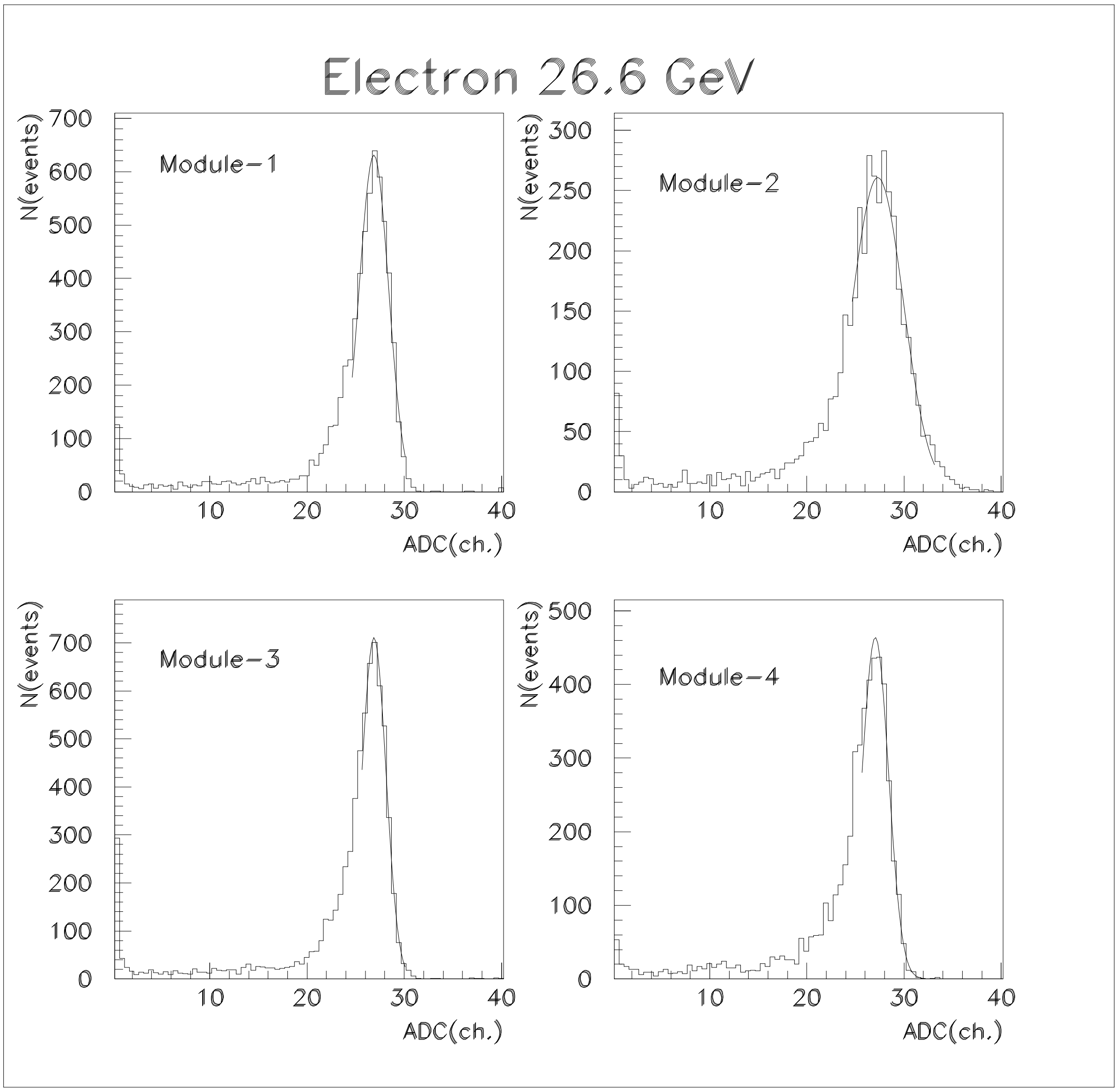

Fig.12. Pulse height distribution for electrons $E = 26.6 \pm 1.1\ GeV$. (Total energy losses for 4 modules)

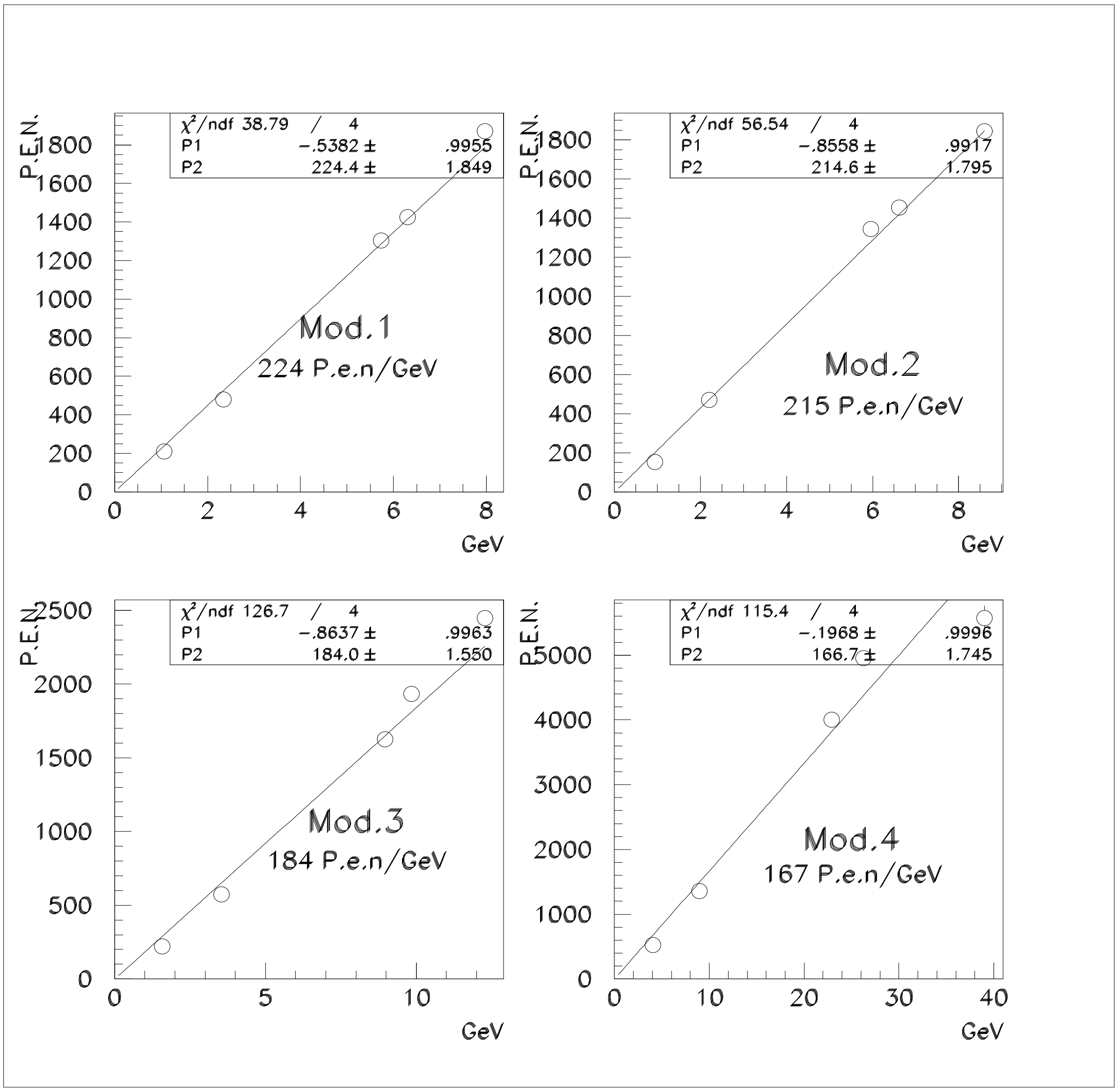

Fig.13. LED calibration of the SP modules in a number of photo–electrons.

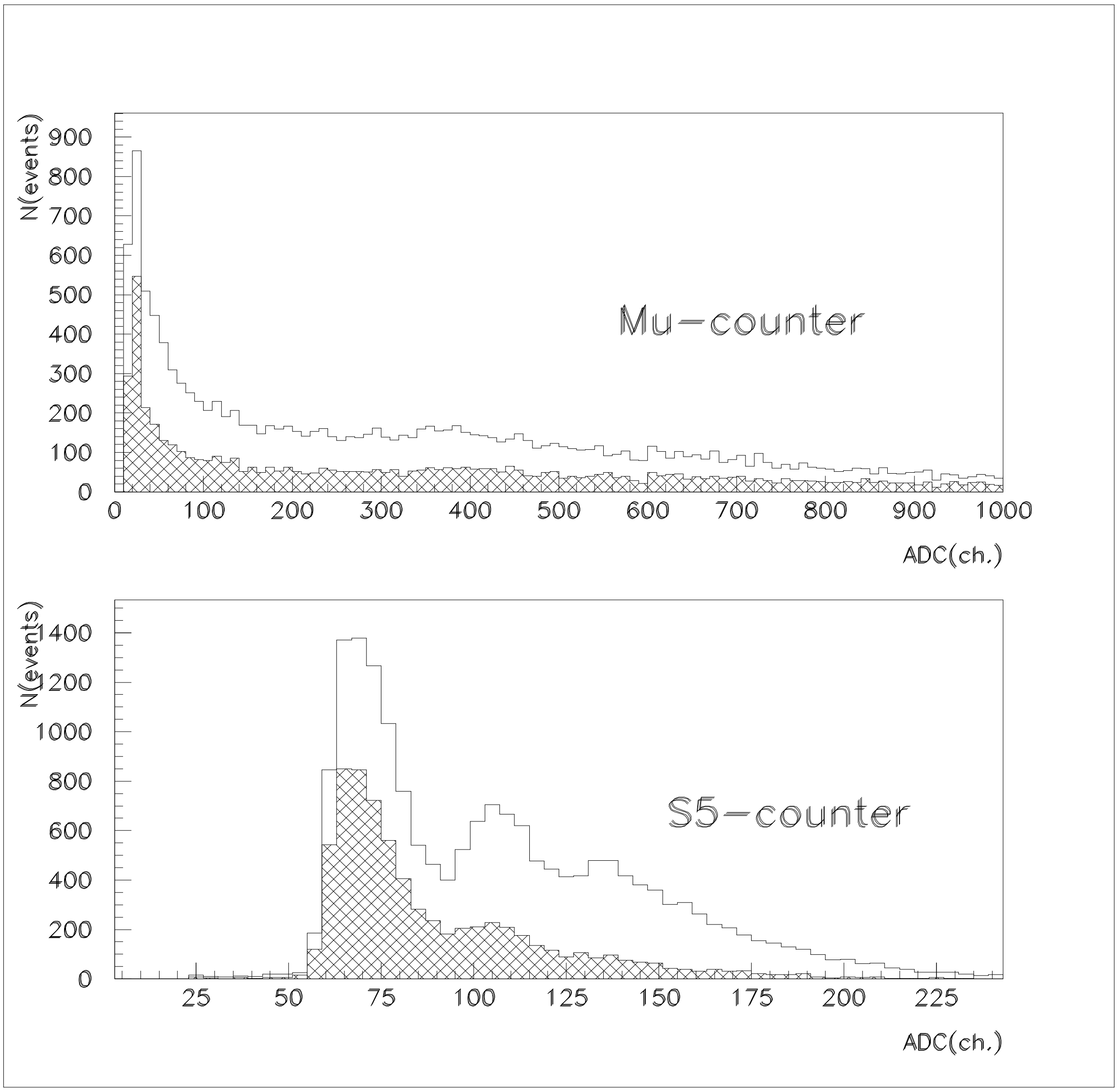

Fig.14. Pulse height distributions for electrons from $S_{\mu}(a)$ and $S_5(b)$ counters with multiplicity of tracks equal 4 (light histogramms) and 1 (dark histogramms).

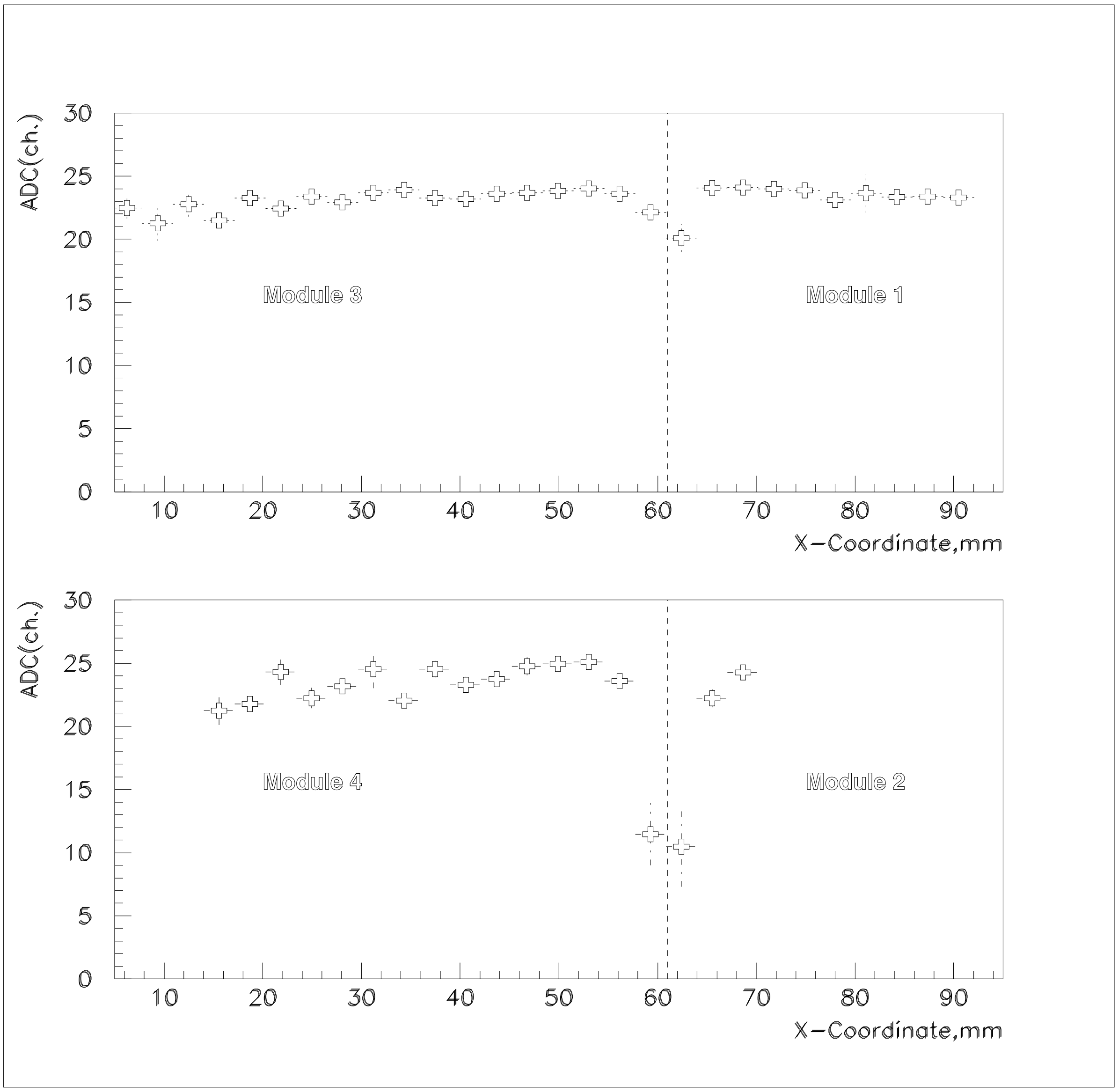

Fig.15. Results of the modules scanning with muons:

a) – for modules $4+2$, the gap between them is equal 6 mm;

b) – for modules $1+3$, the gap between them is equal 1.2 mm.

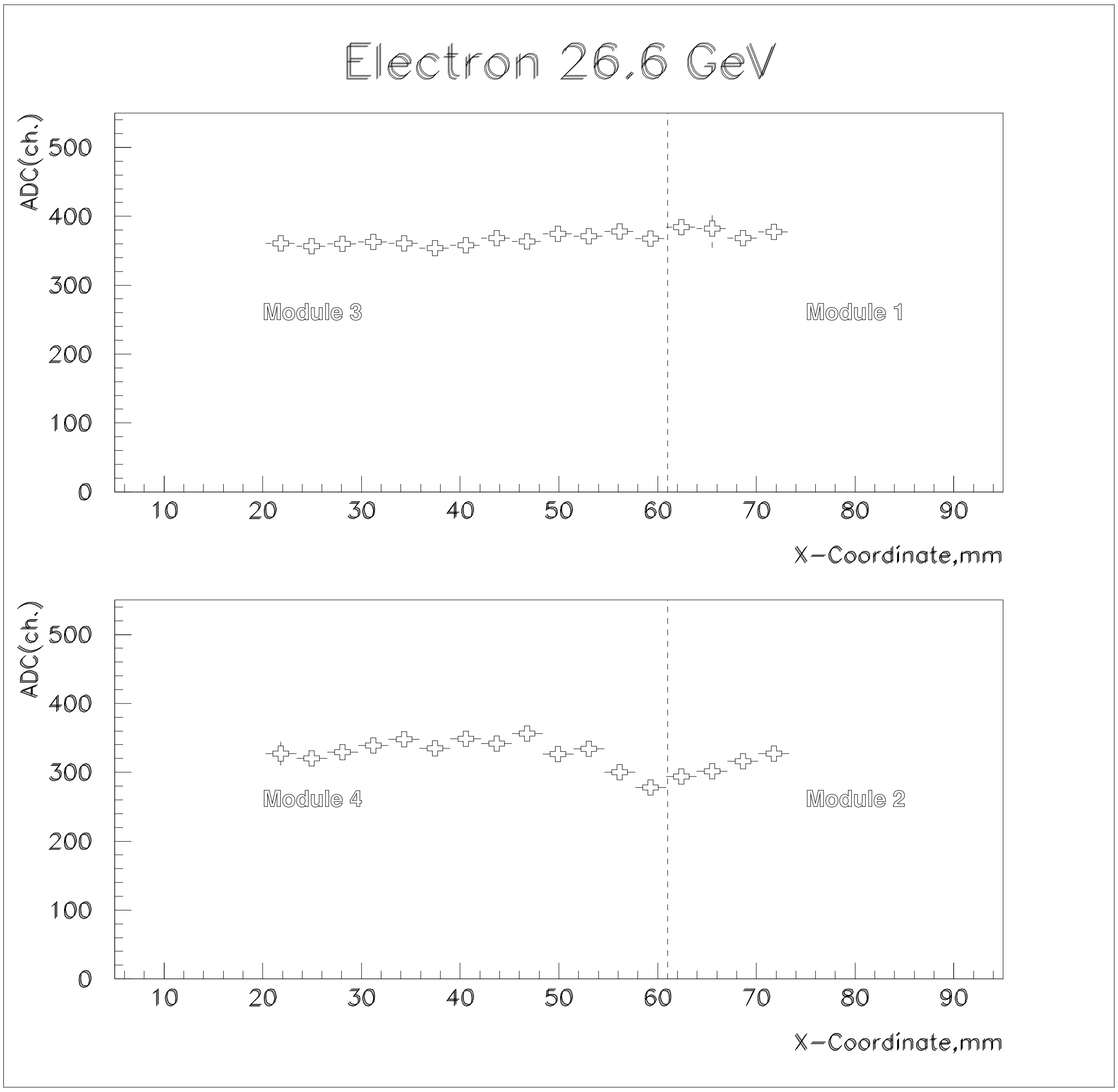

Fig.16. The same as Fig.15 but for the modules scanning with electrons.

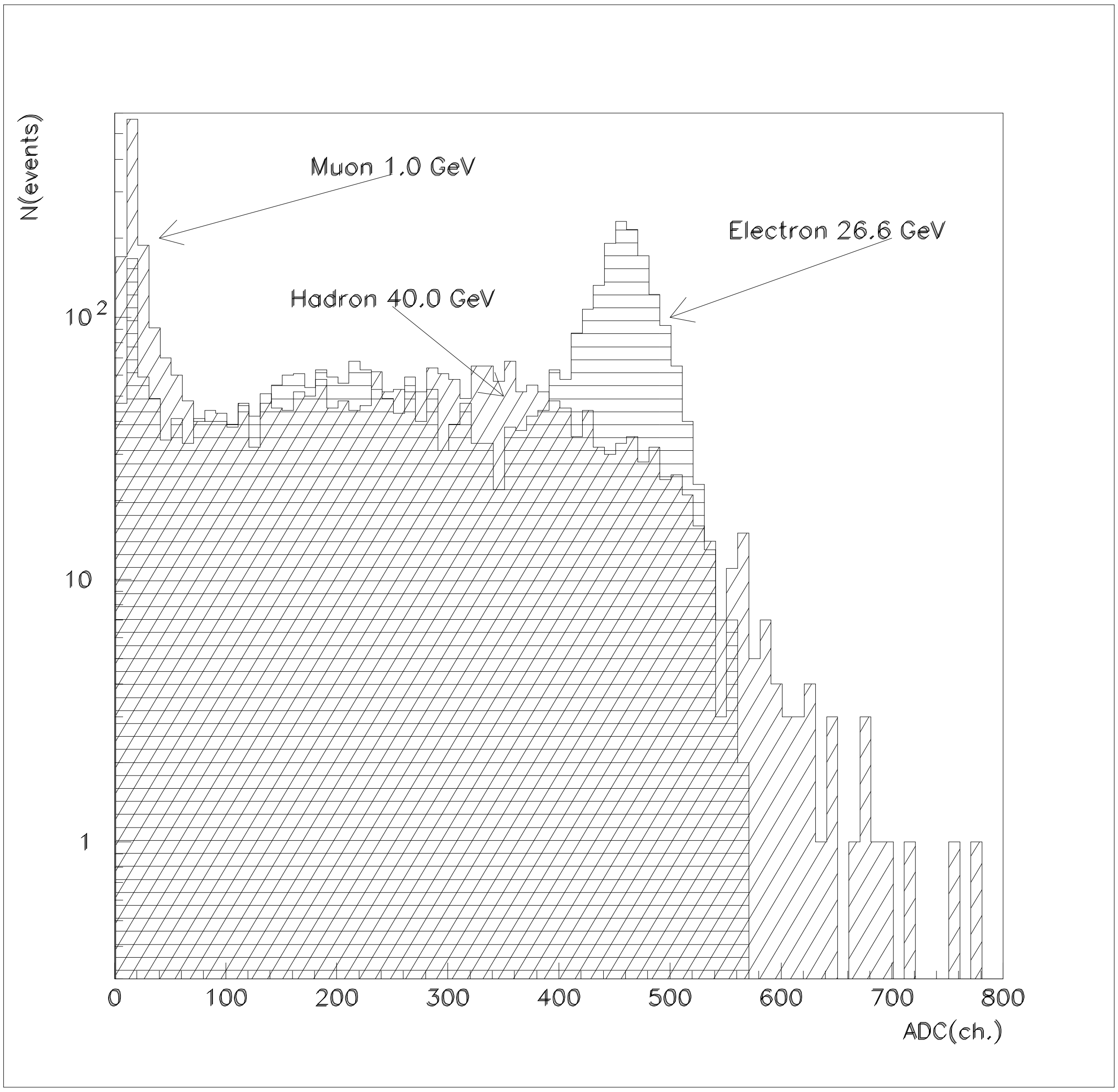

Fig.17. Normalized pulse height distributions for one module obtained with electrons, pions and muons.

List of the tables

Table 1: **Scintillators counter locations**

Counters	Size	Arrangement
S_1, S_2	$10 \times 10 mm^2$	Located at the head of the channel
S_3	$50 \times 50 mm^2$	Located at 6 m from SP
S_A (veto)	$300 \times 300 mm^2$	Located in front of SP
S_5	$50 \times 50 mm^2$	Located in front of SP
S_μ	$100 \times 100 mm^2$	Located after each module of SP

Table 2: **The results of photo–electron number estimations**

WLS, Length, cm	Module 1 Y11, 210	Module 2 BCF91A(s.c.), 150	Module 3 BCF91A(m.c.), 150	Module 4 BCF91A(s.c.), 180
N_{pe} in μ beam, total	70±2	65±3	57±2	55±2
N_{pe} per tile	2.8±0.4	2.6±0.6	2.3±0.4	2.2±0.4

Table 3: **Energy resolution of the SP modules, Photostatistic**

WLS-length (cm.)	Module 1 Y-11-210	Module 2 BCF91A(s.c.)-150	Module 3 BCF91A(m.c.)-150	Module 4 BCF91A(s.c.)-180
σ_E/E,%	5.5±1.2	9.2±1.2	4.7±0.6	4.6±1.0
$\sigma_E/\sqrt(E)$,%	28.3±3.1	47.3±6.2	24.2±3.1	23.7±5.1
N_{pe} e-beam E=26.6 GeV	5958±52	5719±52	4894±52	4442±52
N_{pe} per 1 GeV	224±2	215±2	184±2	167±2

Table 4: **Average amplitude deviations for the SP modules near the dead areas**

	Module 1 + Module 3 gap 1.2 mm	Module 2 + Module 4 gap 6.0 mm
$\frac{A_{min}-A}{<A>}$ on μ-beam	(22±5)%	(56±13)%
$\frac{A_{min}-A}{<A>}$ on e-beam	(3±3)%	(12±3)%